Proposal to Jefferson Lab PAC 29

A CLEAN MEASUREMENT OF THE NEUTRON SKIN OF ^{208}Pb THROUGH PARITY VIOLATING ELECTRON SCATTERING

Spokesmen: R. Michaels, P.A. Souder, G.M. Urciuoli

K.A. Aniol, M.B. Epstein, D.J. Margaziotis
California State Univerisity, Los Angeles

P.A. Souder, R. Holmes
Syracuse University

E. Burtin, D. Lhuillier
DSM/DAPNIA/SPhN CEA Saclay

R. Carlini, J.P. Chen, E. Chudakov, K. De Jager, D. Higinbotham, J. Gomez, J. LeRose, R. Michaels, A. Saha, B. Wojtsekhowski
Thomas Jefferson National Accelerator Facility

E. Cisbani, F. Cusanno, S. Frullani, F. Garibaldi, M. Iodice,G.M. Urciuoli
INFN/Rome

R. De Leo
INFN/Bari

R. Wilson
Harvard University

(over)

C.J. Horowitz
Indiana University

G.D. Cates
Princeton University

K. Kumar, K. Paschke
University of Massachusetts

P. Markowitz
Florida International University

J. Calarco, W. Hersman
University of New Hampshire

T. Averett, D. Armstrong, J.M. Finn, T. Holmstrom, V. Sulkosky
College of William and Mary in Virginia

P. Decowski
Smith College

(This is a Hall A Collaboration Proposal)

Postscript copy of the proposal and the two updates are at http://hallaweb.jlab.org/parity/prex

ABSTRACT

The difference between the neutron radius R_n of a heavy nucleus and the proton radius R_p is believed to be several percent. This neutron skin has proven to be elusive to pin down experimentally in a rigorous fashion. The proposed Lead Radius Experiment PREX will measure the parity-violating electroweak asymmetry in the elastic scattering of polarized electrons from ^{208}Pb at an energy of 850 MeV and a scattering angle of 6°. Since the Z_0 boson couples mainly to neutrons, this asymmetry provides a clean measurement of R_n with a projected experimental precision of ± 1 %. In addition to being a fundamental test of nuclear theory, a precise measurement of R_n pins down the density dependence of the symmetry energy of neutron rich nuclear matter which has impacts on neutron star structure, heavy ion collisions, and atomic parity violation experiments.

Proposal Update: ^{208}Pb Parity

This is an update on proposal E00003, later re-numbered E03011, and entitled "A Clean Measurement of the Neutron Skin of ^{208}Pb Through Parity Violating Electron Scattering" which has come under 3-year jeopardy for the second time. We update the scientific case, the collaboration status, and technical developments needed to perform the experiment. We are requesting 30 days at 50 μA and 850 MeV.

The original proposal will be attached. The proposal as well as this update and the previous update are all available on the experiment's web site: http://hallaweb.jlab.org/parity/prex

I INTRODUCTION

In a heavy nucleus like ^{208}Pb the difference between the neutron radius R_n and the proton radius R_p is believed to be several percent. This neutron skin has not been well established experimentally in stable nuclei. We plan to measure the neutron charge radius R_n (i.e. the RMS radius of neutrons in a nucleus) in a clean and model independent way analogous to the classic measurements [1] of the proton radius R_p and with unprecedented accuracy as suggested originally by Donnelly, Dubach, and Sick [2]. Experimentally R_n is rather poorly known [3]. There is some controversy about exactly how accurately R_n has been measured – probably 5%. Indeed the best estimates of R_n appear to come from nuclear theory [4], where models have been constrained primarily by data *other than* neutron radii. Therefore, a measurement of R_n will provide a powerful independent check of these models.

The experiment measures the parity violating asymmetry in elastic scattering $A = (\sigma_R - \sigma_L)/(\sigma_R + \sigma_L)$. This asymmetry arises due to the the interference of the Z^0 boson amplitude of the weak neutral interaction with the photon amplitude. The asymmetry is sensitive mainly to the neutron radius R_n because the weak charge of the neutron is much larger than that of the proton. In PWIA, the relationship between the asymmetry and the neutron form factor is given by equation (1)

$$A_{LR} = \frac{G_F Q^2}{4\pi\alpha\sqrt{2}}\left[1 - 4\sin^2\theta_W - \frac{F_n(Q^2)}{F_p(Q^2)}\right] \qquad (1)$$

where G_F is the Fermi constant, $\alpha = \frac{1}{137}$ is the fine structure constant, θ_W is the Weinberg angle, and $F_n(Q^2)$ and $F_p(Q^2)$ are the neutron and proton form factor of the nucleus. Thus A_{LR} is approximately proportional to the ratio of neutron to proton form factors. In the above we used PWIA to illustrate. To achieve 1% accuracy requires corrections for Coulomb distortions, which have been calculated by Horowitz [5].

II UPDATE ON THE SCIENTIFIC CASE

In recent years, numerous publications have shown a sustained scientific interest in this proposal. It is remarkable that a single measurement of R_n with 1% accuracy can have such a broad impact on several areas of physics, including neutron star formation and structure [6], atomic parity violation [7,8], nuclear theory [3], and and heavy ion collisions [9]. Indeed, Ref. [3] has been cited 61 times as listed in SPIRES.

From a theoretical perspective, the difference between our proposed measurement of R_n and the well-measured proton radius R_p is determined by fundamental parameters of bulk nuclear matter called the symmetry energy S_ν and the density dependence of the symmetry energy S'_ν. These parameters are important for other phenomena involving nuclear matter, such as heavy ion collisions. Today, perhaps the most important application is the field of supernovae and the properties of neutron stars. The proposed measurement of R_n to 1% will provide the best determination of the S_ν and S'_ν at the density of ordinary nuclear mater. This will provide vital input to the dynamics of stellar explosions and thus have implications for our understanding of how the heavy elements in our world were produced.

The relevant part of the energy of nuclear matter of density n and ratio x of protons to neutrons may be written

$$E(n,x) = E(n,x=1/2) + S_\nu(n)(1-2x^2).$$

The connection between $S_\nu(n_0)$, where n_0 is the density of Pb, our measurement, and R_n is shown by Furnstahl [10] within the context of realistic nuclear calculations. The model dependence of the relations is small compared to our required sensitivity.

The importance of the symmetry energy S_ν for the formation and structure of neutron stars is given in several review articles [11,12]. A good introduction for the non-specialist by Lattimer and Prakish [13] appeared in Science. Neutron stars are giant nuclei $\sim$13 km in diameter, fascinating objects for which astronomical data are rapidly improving. Data on neutron stars include radii,

masses, luminosity, temperature, and cooling rates [14]. In addition to their intrinsic interest as newly explored natural phenomena, these stars provide "laboratories" to understand the nature of extremely dense matter. For example, do collapsed stars form "exotic" phases of matter, e.g. strange stars or quark stars ?

A precise measurement of R_n provides a calibration of the equation of state (pressure versus density) of neutron rich nuclear matter, which is an important input for calculating the structure of neutron stars [6]. To rule in or out possible exotic phases of dense matter one needs to combine the high density measurements of neutron stars with low density precision measurements of R_n in nuclei. R_n also has implications for the crust thickness because the transition density for the liquid-solid phase transition depends sensitively on the neutron skin of ^{208}Pb [6]. The proton fraction of neutron rich matter in beta equilibrium depends on the symmetry energy, which is calibrated by R_n. A large symmetry energy favors more protons, and if the proton fraction is high enough then the following "URCA" process can cool neutron stars $n \rightarrow p + e^- + \bar{\nu}_e \;\; ; \;\; p + e^- \rightarrow n + \nu_e$ where the $\nu_e, \bar{\nu}_e$ carry off energy. URCA cooling might explain recent Chandra observations of the neutron star 3C58, a remnant of the supernova seen in the year 1186 that appears to be unexpectedly cold [14]. A neutron skin larger than about 0.2 fm may imply that URCA cooling is possible, while a smaller skin implies it is probably not possible [15].

Heavy ion reactions [16,17,9], including rare isotope beam experiments anticipated from RIA [18], can also pin down the density dependence of the symmetry energy by probing conditions at neutron densities up to 3 times normal nuclear matter density. A combination of our measurement at subnuclear densities and the RIA results will provide useful constraints on nuclear theory.

The impact of an accurate R_n measurement on atomic parity violation (APV) experiments has been analyzed by Pollock *et.al* [3], [8]. Knowledge of R_n at the 1% level is needed for interpreting atomic physics measurements of the Weinberg angle at the level of the Standard Model weak radiative corrections. The most accurate (1% in $Q_{\rm weak}$) measurement of APV was carried out by Wieman and co-workers in atomic cesium ^{133}Cs [19]. Such low energy experiments provide powerful constraints on the standard model [20]. More independent tests of APV are needed at the accuracy of the Cesium experiment. An alternative approach which largely cancels the uncertainties due to difficult atomic structure calculations is to measure ratios of APV amplitudes between isotopes [21]. This is being exploited for example in the Berkeley atomic Yb experiment [22]. However, Fortson *et.al.* [23] pointed out that this technique has an enhanced sensitivity to uncertainties in R_n. A recent analysis

[7] has emphasized the importance of this experiment on the field.

There have been renewed attempts to obtain R_n from hadronic data. A major effort has been devoted to the analysis of proton scattering [24–27]. Clark and Kerr [26] arrive at the smallest claimed error on R_n, less than 1%. Piekarewicz [24] suggests that the error should be at least 3%. Karataglidis et al. [25] suggest that the proton and proposed data are complementary and that both are important. We note that recent data on pion photoproduction from lead and other nuclei [28] have yielded matter radii that are less than the charge radii, implying a *negative* neutron skin in ^{208}Pb.

The physics interpretation of the experiment can be summarized as follows. From the measured asymmetry one may deduce the weak form factor, which is the Fourier transform of the weak charge density at the momentum transfer of the experiment. One must correct for Coulomb distortions, which has been done accurately by Horowitz [5] and others [29]. The weak charge density can be compared directly to theoretical calculations and this will constrain the density dependence of the symmetry energy. The weak density can be directly applied to atomic parity violation because the observables have approximately the same dependence on nuclear shape. From the weak charge density one can also deduce a neutron density at one Q^2 by making small corrections for known nucleon form factors. The uncertainty in these corrections for a realistic experiment have been estimated and are small [3]. The corrections considered were Coulomb distortions (which was by far the biggest), strangeness and the neutron electric form factor, parity admixtures, dispersion corrections, meson exchange currents, isospin admixtures, radiative corrections, and possible contamination from excited states and target impurities.

Finally from a low Q^2 measurement of the point neutron density one can deduce R_n. This requires knowledge of the surface thickness to about 25% to extract R_n to 1%. The spread in surface thickness among successful mean field models is much less than 25%, hence we can extract R_n with the desired accuracy as shown by Furnstahl [10]. In summary, the physics results of the experiment are the weak charge density, the point neutron density and R_n.

III EXPERIMENTAL OVERVIEW

Since the original proposal the experiment has not changed. In this section we provide a brief overview of the experiment. In subsequent sections we discuss the main technical problems and the progress or plans for solving them.

The experiment uses a beam energy of 850 MeV and a 6° scattering angle in Hall A using the two HRS spectrometer systems supplemented by septum

TABLE 1. Acceptance Averaged Rate and Asymmetry

Measured Asymmetry (p_e A)	0.51 ppm
Beam Energy	850 MeV
Beam Current	50μA
Required Statistical Accuracy	3%
Energy Cut (due to detector)	4 MeV
Detected Rate (each spectrometer)	860 MHz
Running Time	680 hours

magnets which focus elastically scattered electrons onto total-absorption detectors in their focal planes. A 50μA, 80% polarized beam with a 30 Hz helicity reversal will scatter from a foil of lead which is sandwiched between sheets of diamond to improve the thermal characteristics. Ratios of detected flux to beam current integrated in the helicity period are formed, and the parity–violating asymmetry in these ratios computed from the helicity–correlated difference divided by the sum: A = (σ_R - σ_L) / (σ_R + σ_L), where $\sigma_{R(L)}$ is the ratio for right(R) an left(L) handed electrons. Separate studies at lower rates are required to measure backgrounds, acceptance, and Q^2. Polarization measurements by Møller and Compton polarimetry are discussed in section VF.

Table 1 shows the rates, asymmetries, and running time for the ^{208}Pb parity experiment proposal.

IV COLLABORATION STATUS

The experiment remains a Hall A collaboration proposal, and the core experimental group is the HAPPEX collaboration which has completed three published parity experiments in Hall A since 1998 [30]. In addition, several collaborators were central to the the SLAC parity experiment E158 [31]. These experiments have provided valuable experience and have tested many aspects of the Lead parity experiment as explained below. The collaboration list on the front cover is up-to-date, with some additions and subtractions from three years ago.

V TECHNICAL UPDATE

The major technical problems of this experiment can be divided into the following categories. A) Helicity Correlated Systematic Errors; B) Q^2 Measurement; and C) High Power Target Design; D) Noise Levels; E) Septum Magnet; F) Precision Polarimetry. Due to recent progress, items A) - C) are well under control. For items D) - F) we provide specific plans to solve the problems within the next two years.

For the ^{208}Pb experiment the asymmetry of 0.5 ppm must be measured to 3% accuracy. Both the absolute error (15 ppb) and the relative accuracy (3%) are challenging to achieve. The main issues affecting the absolute error are the control of false asymmetries associated with helicity correlations in beam parameters such as intensity, energy, and position. The main issues affecting the relative error are the beam polarimetry and measurement of Q^2.

A Helicity Correlated Systematics

To evaluate the systematic error we need to know the helicity correlated differences as well as our sensitivity to these which are measured online by modulation of the parameters. During the 2005 HAPPEX run we have made tremendous progress in controlling helicity correlated systematics, see fig 1 which shows 1-month averages of $\sim$1 nanometer in helicity correlated position differences. This accomplishment is due to a long-term effort to improve the setup of the polarized source and accelerator. For the polarized source we have a well-developed model for controlling the laser systematics, which allows us to minimize helicity correlations in the laser beam used to produce polarized electrons. For the accelerator, progress in understanding the betatron matching has helped achieve maximum dampening of position differences, while improved understanding of beam tuning has provided both excellent signal-to-noise ratios in the Compton polarimeter and good phase advances along our beamline that permit us to simultaneously have good measurements to the sensitivities of each of the independent beam parameters. For ^{208}Pb we want to maintain position differences to less than 1 nm with an accuracy of 0.1 nm averaged over a 1 month run. The charge asymmetry must be maintained to less than 100 ppb with an accuracy of 10 ppb.

Experience from the SLAC experiment E158 is also relevant to this proposal. Data published by the E158 group [31] provided a measurement below the 20 ppb level. The systematic uncertainties due to helicity-correlated beam parameters were shown to be significantly below this level.

Our sensitivity to beam parameters (slopes) are measured online and in situ by modulating the beam position, angle, and energy. Because of the sharply falling form factor, lead is expected to be more sensitive than HAPPEX-He or HAPPEX-H. We believe the helicity correlated position differences we've obtained are adequate for lead. We have performed these measurements during a test of our lead target at 1.1 GeV, see also the next section. We found that the lead slopes were comparable in magnitude to the slopes measured during HAPPEX in 2005. Based on these measurements and the expected improved performance of the cavity position monitors, we expect that the contribution of electronics noise will be small compared to statistics.

We have installed and commissioned new microwave cavity beam position and current monitors. These new monitors supplement the existing stripline monitors and provide potentially greater accuracy as well as a complementary method with different systematics. In addition they provides an important redundancy necessary to unfold beam fluctuation noise from instrumentation noise. This redundancy will also be useful for establishing helicity correlated differences at the sub-nanometer level in a convincing fashion. Fig. 2 shows preliminary analysis of data on the correlation of cavity to stripline position differences from our 2005 HAPPEX data. An approximate run-averaged calibration was used for the cavity monitors in this analysis. The good correlation and the average agreement at the few nanometer level is encouraging, but the cavities still suffer from subtle problems like cross-talk which we plan to solve parasitically in the upcoming year. Our solutions to the problems include: 1) The reliability of the electronics was affected by radiation, so we will move the electronics to a well shielded area to reduce the chance of the phase lock loop losing its lock. 2) We need to learn about the apparent cross talk between channels to see if better isolation of the electronics is necessary or if higher modes are present in the cavities. 3) Stabilize the phase reference to reduce the noise. 4) Increase the sensitivity at low currents (50 nA), necessary for counting mode tests.

B Lead Target Tests

We have successfully tested our lead target at 80μA, thus proving that the design in our original proposal works. We have built a high power lead target which will be stable at 40 Watt for a 50 μA beam. Beam tests at 80μA, as well as calculations, show that we have a good target design.

Recently we have performed low-intensity tests at 1.1 GeV, which is approximately the energy of this proposal. The purposes of the run were to check the rates, backgrounds, resolution, sensitivity to beam parameters (slopes), and

width of asymmetry. Figs 3 and 4 show the elastic peak in the HRS focal plane. The first excited state (2.6 MeV) may be cleanly resolved by an integrating detector; furthermore, it is a small background (expected $\sim$0.1%) and is not visible here. The rates in counting mode were 1.5 times higher than the predicted rate; however, this is within the error of beam current at the very low currents (0.1 μA) where we had to run to avoid significant deadtime. The width of the asymmetry in integrating mode for beam current 1 to 4 μA was consistent with the counting mode rate and scaled with current I as $1/\sqrt{I}$. The events are very clean and background-free, as it was for HAPPEX, a good characteristic of the HRS environment.

C Normalization Error due to Q^2

The limitation in measuring Q^2 was the knowledge of the spectrometer angle, which until recently was about 1 mrad due to difficult surveys. We still perform such surveys as a cross check; however, during HAPPEX-2 we have developed a new method using the energy recoil from nuclei [32] to measure the scattering angle with accuracy $\pm 0.02^\circ$ which provides an accuracy of $\pm 0.7\%$ in Q^2 which is adequate for this proposal.

D Noise

The pulse-to-pulse noise in the lead experiment is 140 ppm. A similar noise level has been achieved during the SLAC experiment E158 [31]. All other noises must be small compared to 140 ppm in order for counting statistics to dominate our errors and to keep the running time minimal. It will be important to avoid long cable runs for our detectors, and therefore we have installed a distributed DAQ system during HAPPEX-2, in which the DAQ crates are situated near the detectors.

For understanding the noise, beam systematics, and possible target boiling effects, we have implemented a new luminosity monitor in 2003 which was used during HAPPEX-2. These monitors consist of quartz Cherenkov detectors located at small angle near the beam after the target. The quartz is a radiation hard material, cut and polished into rectangular bars attached via a light guide to well-shielded PMTs. There are two monitor stations, one at a "larger" angle (6°) at a very small angle (0.5°). The stations at a larger angle sees an extremely high rate. This is useful to measure the baseline electronics noise of the system, as it is difficult to measure sub-100 ppm electronics noise and preferable to use a physical signal. A second part of the monitor is at the

smaller angle and sees higher energy particles and is primarily sensitive to the beam parameters (position, angle). The small–angle monitor is segmented to unfold the beam parameters.

New 18-bit ADCs are being fabricated at JLab for use in upcoming parity experiments. These will improve the pedestal noise and will replace our obsolescent 16-bit ADCs. The improved noise level is accomplished by a combination of the increased bit resolution and by a sampling technique on the ADC board that was developed at E158.

E Septum Magnet

The existing superconducting septum magnets in Hall A will not work at the high luminosity of our experiment due to beam induced radiational heating of the superconducting coils. Since this experiment requires less than half the magnetic field in the septum that other experiments running at higher energies, an inexpensive normal conducting septum magnet with lower full field has been designed. This magnet will be much more robust with respect to heat loads than the superconducting septa. The design has been magnetostatically designed using TOSCA and resulting maps of the expected magnetic fields have been used in a raytracing study to ensure that the hardware resolution needed to separate the elastic peak in lead from the first excited state will be achieved. In fig. 5 the distribution at the spectrometer focus of two monochromatic bundles of trajectories with $\frac{dp}{p} = 0$ and -0.35% ($\sim$3 MeV/c at 850 MeV/c) respectively are shown. This shows we can resolve the first excited state (2.6 MeV) of lead. The two bundles are always more than 2 cm apart which is an adequate spatial resolution for the integration technique.

F Precision Polarimetry

Improvements in polarimetry are of vital importance for the Jefferson Lab parity violation program. High accuracy (sub-1%) is important not only for this proposal but for the $Q_{\rm weak}$ proposal [E05-008], the DIS parity [E05-007], DIS parity at 12 GeV, and HAPPEX-III [E05-009]. For this proposal, the polarization must be measured to 1% preferably, or at least 2%. With a polarization accuracy of 1% (2%) we can extract R_n to 1% (1.2%) respectively. Here we formulate our specific strategy to address this issue. Our plan is to use a combination of upgraded Compton polarimeter and upgraded Møller polarimeter.

The best accuracy obtained so far with the Compton polarimeter is 1.5% total relative error within 40 minutes for a beam energy of 4.5 GeV. We plan to implement a green laser to improve the figure of merit at 850 MeV. This brings the mean asymmetry to 0.65%. At the Compton edge the photon energy is 26 MeV and the associated scattered electron is 6 mm above the primary beam at the location of the electron detector. Assuming the same laser power of 1.5 kW at the Compton interaction point, a 1% statistical accuracy is achieved within 16 hours. The laser and much of the associated optics equipment has been obtained and is undergoing test. In addition to the laser, we plan on using a new crystal for the photon detector.

A further improvement in Compton polarimetry is to use an integration method. This removes two of the main systematic errors, those due to the response function and the deadtime. In principle, the integration mode should provide a 1% systematic error. A prototype integration mode has been deployed during HAPPEX-2 and shows promise of working well; however, we will need to develop better, i.e. more linear, electronics.

The present Møller polarimeter in Hall A uses for the target several magnetic foils, tilted at 20° to the beam, magnetized in an external field of about 0.025 T. Measurements are invasive and are done at beam currents below 1 μA. The systematic error of about 2% is mainly driven by the uncertainty in the target polarization. It can be reduced to about 1% by using the technique of foil saturation developed in Hall C [33], where an iron foil is positioned normally to the beam direction and magnetized along the beam in a field of ~ 4 T. A working magnet exists and is available from an earlier version of the Hall C polarimeter. This upgrade would allow to reduce the foil polarization error down to about 0.4%, as well as to use a higher beam current of about 3 μA. The latter improves the accuracy of extrapolation to the regular beam current of about 50 μA.

We will compare Møller to Compton at 5 μA and 6 GeV to give a clear comparison at the 1% level.

VI BEAM TIME REQUEST

The original beam time request has not changed. We request 30 days of polarized beam running in Hall A at 850 MeV using the two septum magnets.

REFERENCES

1. H. de Vries, C. W. de Jager, and C. de Vries, Atomic and Nuclear Data Tables, **36**, 495 (1987).
2. T.W. Donnelly, J. Dubach, and I. Sick, Nucl. Phys. **A503**, 589 (1989).
3. C. J. Horowitz, S. J. Pollock, P. A. Souder, and R. W. Michaels, Phys. Rev. C **63**, 025501, (2001).
4. C. J. Horowitz, private communication.
5. C. J. Horowitz, Phys. Rev. C **57**, 3430 (1998).
6. C. J. Horowitz, J. Piekarweicz, Phys. Rev. Lett **86**, 5647 (2001). C. J. Horowitz, J. Piekarewicz, Phys. Rev. C**64**, 062802 (2001). C. J. Horowitz, J. Piekarewicz, atro-ph/0201113 (2002). J. Carriere, C.J. Horowitz, J. Piekarewicz nucl-th/0211015 (2002).
7. T. Sil, M. Centelles, X. Vinas and J. Piekarewicz, Phys. Rev. C **71**, 045502 (2005) [arXiv:nucl-th/0501014].
8. S.J. Pollock, E.N. Fortson, and L. Wilets Phys. Rev. C **46**, 2587 (1992).
9. A. W. Steiner and B. A. Li, Phys. Rev. C **72**, 041601 (2005) [arXiv:nucl-th/0505051].
10. R. J. Furnstahl, Nucl. Phys. **A706**, 85 (2002).
11. A. W. Steiner, M. Prakash, J. M. Lattimer and P. J. Ellis, Phys. Rept. **411**, 325 (2005) [arXiv:nucl-th/0410066].
12. J. M. Lattimer and M. Prakash, Phys. Rept. **333**, 121 (2000) [arXiv:astro-ph/0002203].
13. J.M. Lattimer, M. Prakash, Science 304 (2004) 536.
14. New York Times, April 11, 2002 edition; P. Slane, D. Helfand, S. Murray, astro-ph/0204151; G.G. Pavolv, O.Y. Kargaltzev, D. Sanwal, and G.P. Garmire, ApJ **554**, L189 (2001); J.P. Halpern and F.Y.H. Wang, ApJ. **447**, 905 (1997); M. Colpi, U. Geppert, D. Page, and A. Possenti, ApJ. **553**, 382 (2001); D. G. Yakovlev *et.al.* astro-ph/0204233.
15. J. Piekarewicz, nucl-th/0207067 (2002).
16. A. Ono, P. Danielewicz, W. A. Friedman, W. G. Lynch and M. B. Tsang, Phys. Rev. C **70**, 041604 (2004) [arXiv:nucl-th/0409027].
17. D. V. Shetty *et al.*, Phys. Rev. C **70**, 011601 (2004) [arXiv:nucl-ex/0406008].
18. B. A. Li, Phys. Rev. C **69**, 034614 (2004) [arXiv:nucl-th/0312025].
19. C. S. Wood *et.al* Science **275**, 1759, (1997) S.C. Bennet and C.E. Wieman, Phys. Rev. Lett. **82**, 2484 (1999).
20. M.-A. Bouchiat and C. Bouchiat, Rep. Prog. Phys. **60**, 1351 (1997).
21. A. Derevianko and S.G. Porsev, physics/0112035 (submitted to Phys. Rev. A) (2002).
22. D. DeMille, Phys. Rev. Lett **74**, 4165 (1995), C.J. Bowers, *et.al* Phys. Rev. **A53**,(5), 3103 (1996); Phys. Rev. A **59**, 5 (1999)
23. E.N. Fortson, Y. Pang, and L. Wilets, Phys. Rev. Lett. **65**, 2857 (1990).
24. J. Piekarewicz and S. P. Weppner, arXiv:nucl-th/0509019.
25. S. Karataglidis, K. Amos, B. A. Brown and P. K. Deb, Phys. Rev. C **65**, 044306 (2002) [arXiv:nucl-th/0111020].

26. B. C. Clark, L. J. Kerr and S. Hama, Phys. Rev. C **67**, 054605 (2003) [arXiv:nucl-th/0209052].
27. M. Dupuis, S. Karataglidis, E. Bauge, J. P. Delaroche and D. Gogny, arXiv:nucl-th/0506077.
28. B. Krusche, arXiv:nucl-ex/0509003 Sept 2005
29. See refs in [3], Relativistic Optical Code RUNT, E.D. Cooper, Los Alamos preprint nucl-th/9911024, D. Vretenar *et al.*, and calculations by B.C. Clark *et al.*.
30. K. A. Aniol *et al.*, Phys. Rev. Lett. **82** 1096 (1999). K. A. Aniol, *et al.*, Phys. Rev. C 69, 065501 (2004). K. A. Aniol, *et al.*, nucl-ex/0506010. K. A. Aniol, *et al.*, nucl-ex/0506011.
31. P.L Anthony, *et.al.* Phys.Rev.Lett.95:081601,2005.
32. T. Holmstrom, R. Feuerbach, R. Michaels, "Q^2 for HAPPEX-2" technical report http://hallaweb.jlab.org/experiment/HAPPEX/docs/qsq_2004.ps
33. M. Hauger *et.al.* Nucl. Instrum. Meth. A**462** 382 (2001).

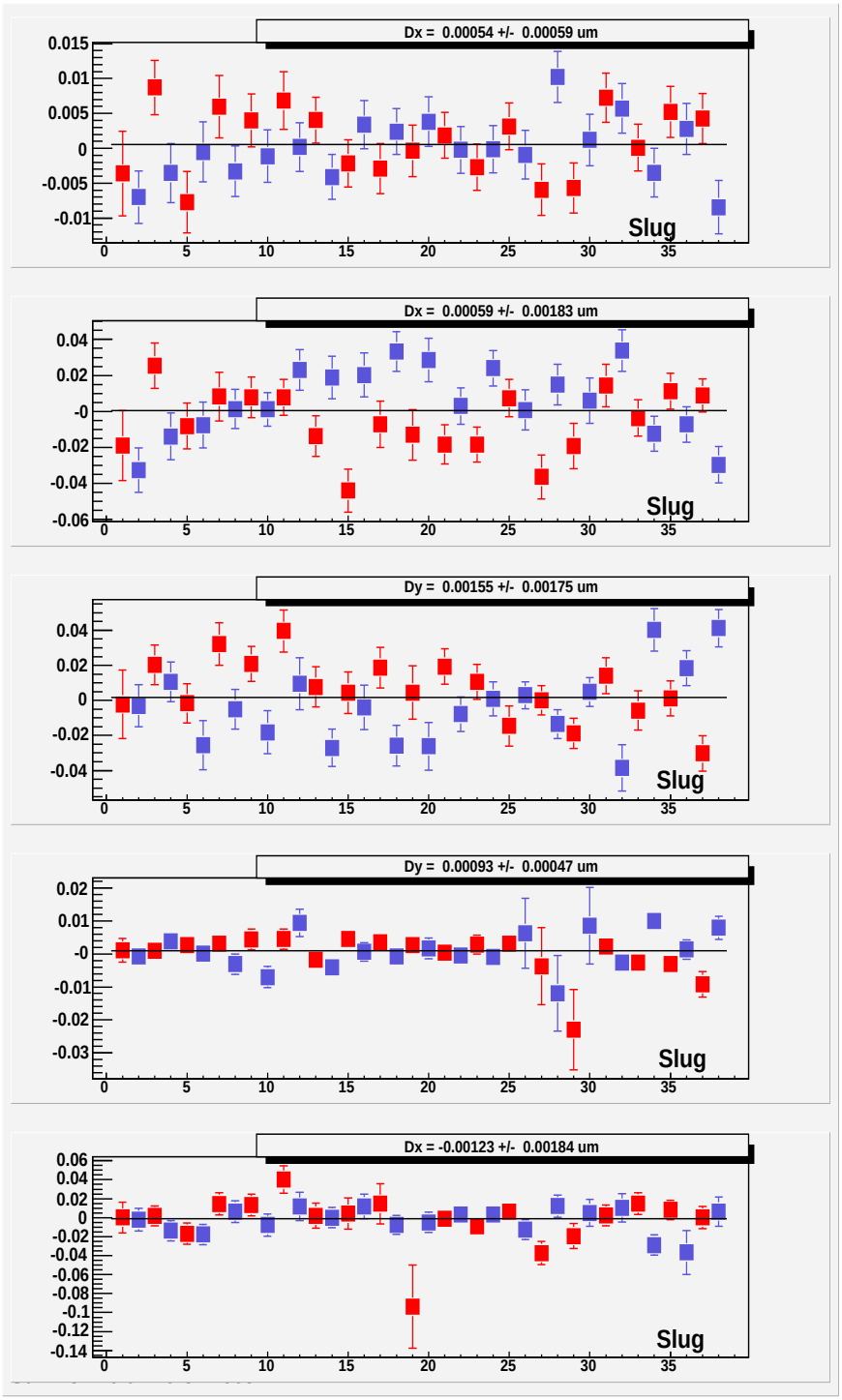

FIGURE 1. Helicity correlated beam monitor differences (μm) versus slug number (1 "slug" $\sim$ 1 day of running) for HAPPEX-2. The top four plots are X and Y monitors near the target, and the bottom plot is a monitor in the dispersive section of the magnet ARC leading into the hall, providing a relative energy monitor. The averages over a month of running are $\sim$ 1 nanometer.

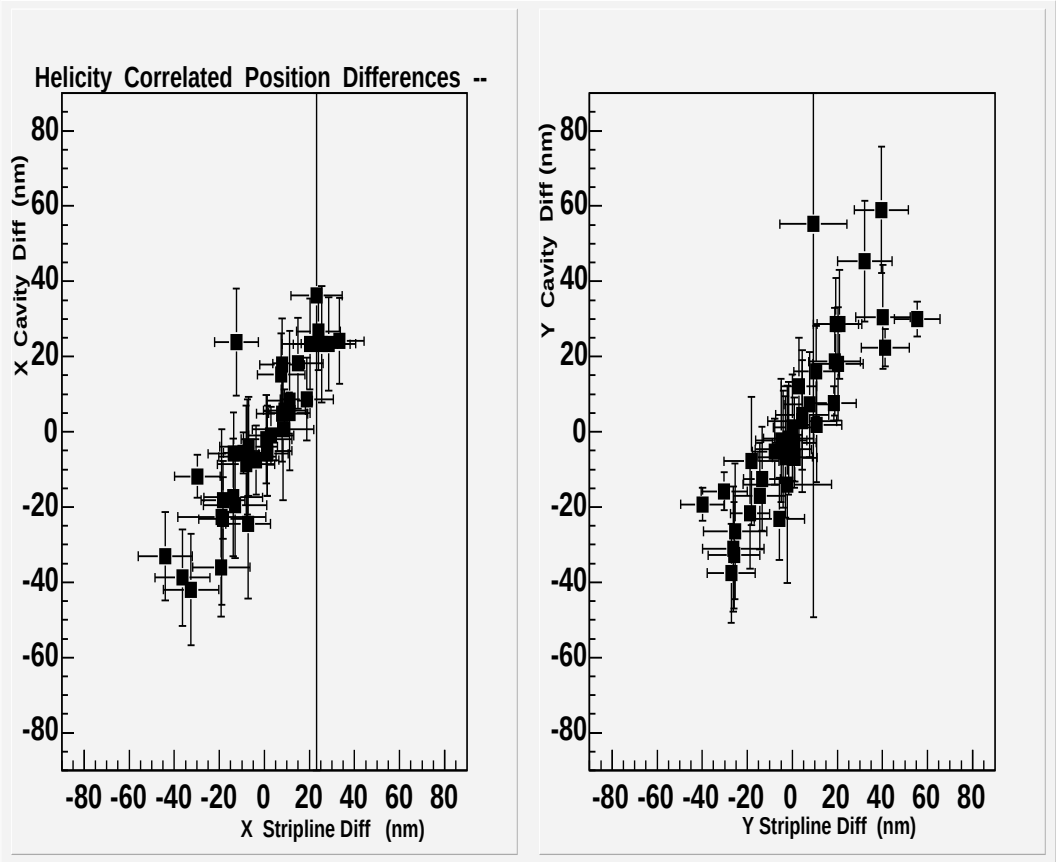

FIGURE 2. Helicity correlated position differences in microwave cavity monitors versus stripline monitors for the horizontal (X) and vertical (Y) directions during the HAPPEX 2005 Hydrogen run. Each point is about 1 day of running. The averages are near zero and agree at the level of a few nm.

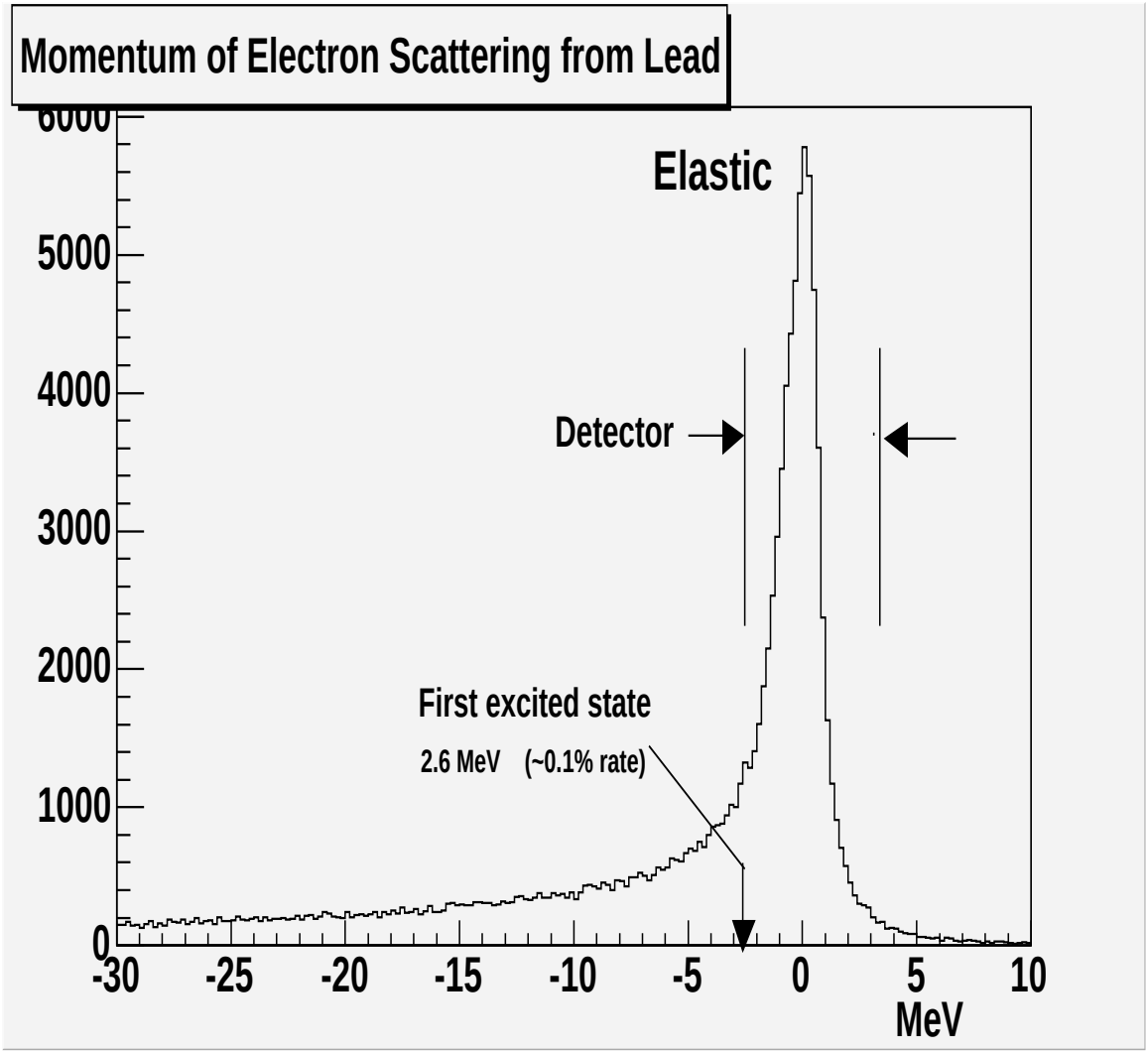

FIGURE 3. Data from our 2005 test run with lead target. The momentum spectrum of the elastic peak, showing the extent of the detector to discriminate possible inelastic levels. The 1st state is at 2.6 MeV and is $\sim$0.1% of our rate.

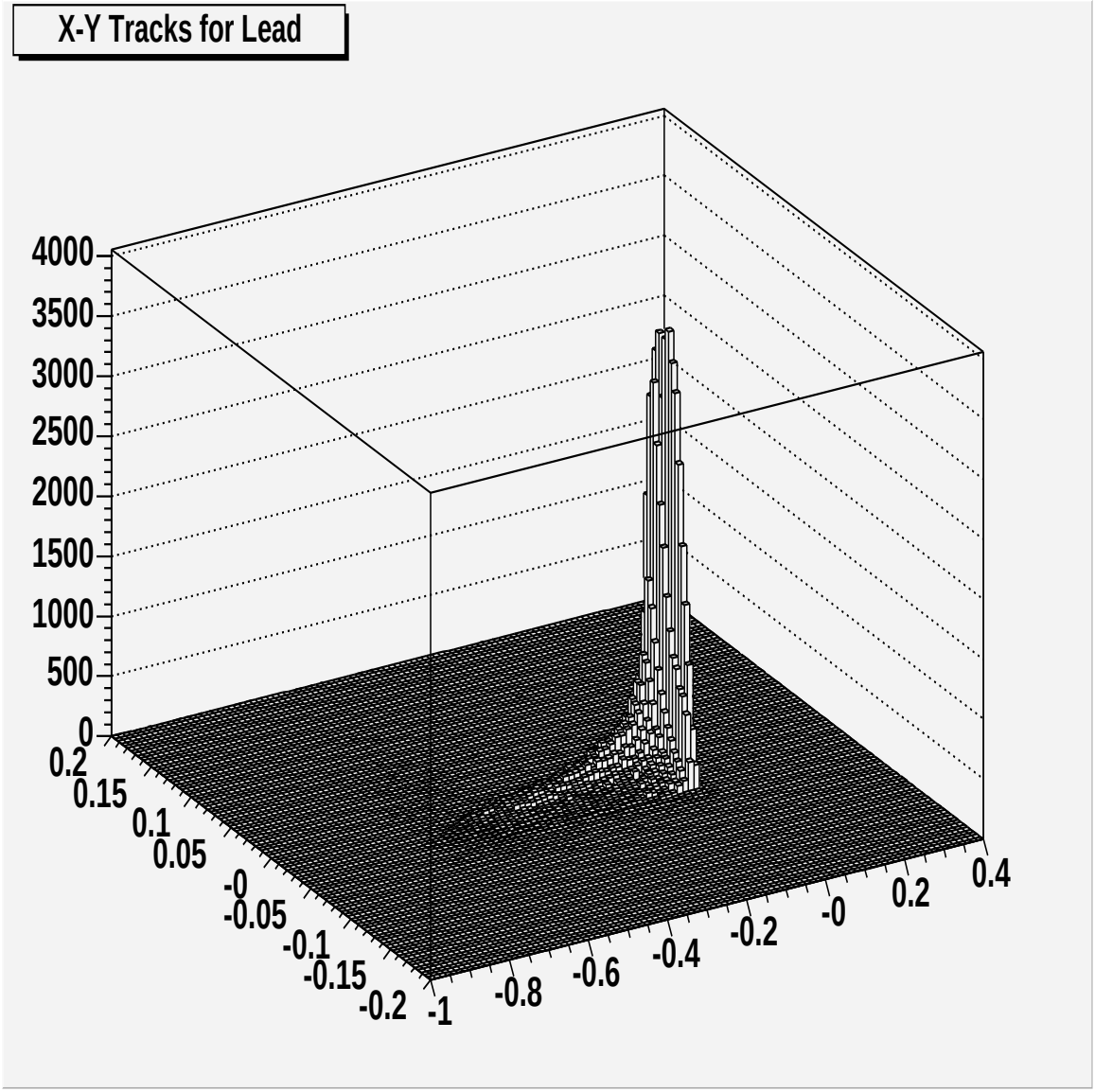

FIGURE 4. Data from our 2005 test run with lead target. The spatial distribution (units are meters) of tracks in the focal plane showing a clean background-free elastic peak.

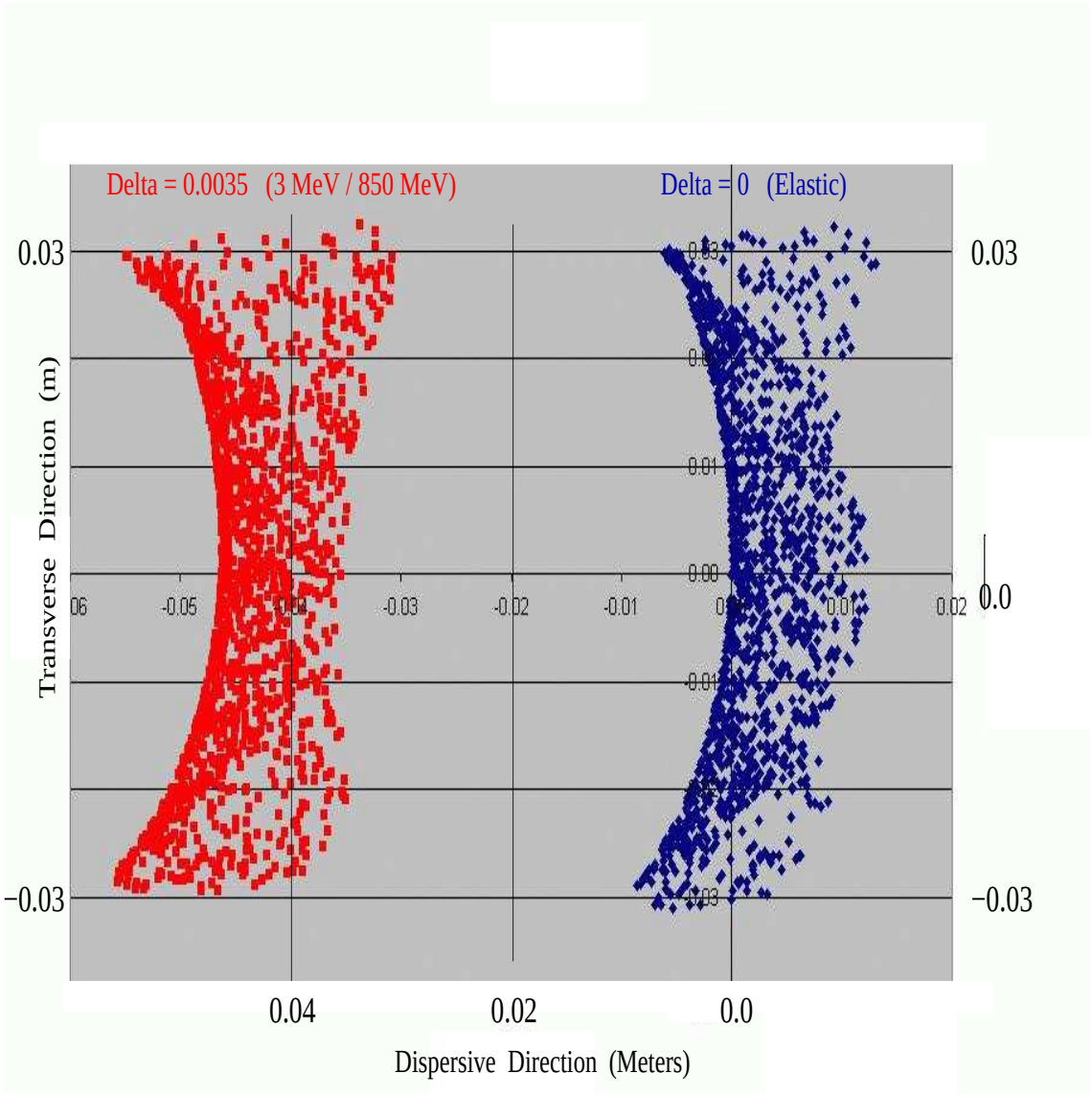

FIGURE 5. Simulated resolution of a warm low energy septum design. Distribution at the spectrometer focus of two monochromatic bundles of trajectories separated by 3 MeV/c at 850 MeV/c are shown, leading to spatial separations of $\geq$2 cm.